Heliyon 9 (2023) e21451

Contents lists available at ScienceDirect

Heliyon

journal homepage: www.cell.com/heliyon

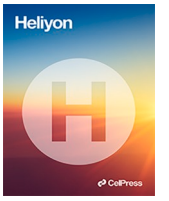

Peristaltic motion of Jeffrey fluid with nonlinear mixed convection

S. Farooq [a,*], T. Shoaib [a], S.Z.B. Bukhari [a], A.S. Alqahtani [b], M.Y. Malik [b], S. Abdullaev [c,d], S.E. Alhazmi [e]

[a] Department of Mathematics and Statistics, Riphah International University I-14, Islamabad 44000, Pakistan
[b] Department of Mathematics, College of Sciences, King Khalid University, Abha, 61413, Saudi Arabia
[c] Senior Researcher, Faculty of Chemical Engineering, New Uzbekistan University, Tashkent, Uzbekistan
[d] Senior Researcher, Department of Science and Innovation, Tashkent State Pedagogical University named after Nizami, Bunyodkor street 27, Tashkent, Uzbekistan
[e] Mathematics Department, Al-Qunfudah University College, Umm Al-Qura University, Mecca, Saudi Arabia

ARTICLE INFO

Keywords:
Jeffrey liquids
Peristaltic motion
Hall phenomena
Non-Darcy porous media
Slip aspects
Chemical reaction and activation energy
Nonlinear
Mixed convection

ABSTRACT

Since previous few decays the consideration of non-Newtonian liquids motion due to its immense usages in medicine, biology, industrial procedures, chemistry of catalysts and in environment. Various studies examine the significance of bio-materials flow in physiological procedures to explore the cure of diagnosed symptoms of disease appearing during movement in a human physiological system. To illustrate the characteristics of physiological liquids various non-Newtonian models have been proposed, but yet no such single liquid model is exploited which describes all the properties of nonlinear behaving liquids. Among these several non-Newtonian models, Jeffery liquid model should be reduced to its base fluid case (i.e. viscous liquid) by choosing $\lambda_1 = \lambda_2 = 0$. Various physiological materials which represents both linear and nonlinear characteristics respectively blood is one of these. Jeffery fluid and peristaltic motion have some common properties such as radii, relaxation time and retardation time. Moreover heat and mass transfer is also an important phenomenon which is suitable for various physiological processes such as hemodialysis and oxygenation etc. Thus due to such motivating facts this research is conducted to investigate the peristaltic motion of electrically conducting Jeffery liquid. The peristaltic propagating channel walls are asymmetric and inclined. Joule heating and magnetic field effects are considered by applying magnetic field in transverse direction to the flow. Further conservation laws modelled the flow situation via considering quadric mix convection, thermos diffusion and diffusion-thermos, heat generation and absorption, chemical reaction with activation energy features. Moreover, creeping flow and long wavelength assumptions are used to simplify the mathematical modelling. The reduced system of equation is solved numerically through built-in technique in Mathematica software. This built-in technique is working through ND Solve command and shooting and RK-Felburg numerical schemes are behind this technique. These numerical results are used to discuss the flow quantities i.e., velocity, temperature and concentration against the sundry dimensionless quantities. Examining the results it comes to know that both thermal and concentration nonlinear mix convection have oppositely affecting the axial velocity. Both heat and mass transfer are escalating function of thermo-diffusion/diffusion-thermo aspects.

* Corresponding author.
E-mail address: farooq.fmg89@yahoo.com (S. Farooq).

https://doi.org/10.1016/j.heliyon.2023.e21451
Received 5 June 2023; Received in revised form 17 October 2023; Accepted 21 October 2023
Available online 23 October 2023

Nomenclature

Symbols	*Interpretation*
$(\overline{X}, \overline{Y})$	Coordinate axes in a fix frame
$(\overline{x}, \overline{y})$	Coordinate axes in a moving frame
h_1, h_2	Wall shaped in a wave frame
J	Joule current
a_1, b_1	Amplitude of upper and lower waves
t	Time
d_1, d_2	Uniform channel width
g	Gravity vector
ρ	Density
κ	Thermal conductivity
C_p	Specific heat
D_B	Brownian motion coefficient
C_s	Susceptibility of concentration
E_a	Energy activation
P	Pressure force
S	Extra stress tensor
A	Rivilin-Ericksen first tensor
σ	Electric conductivity
Ec	Eckert parameter
Br	Brinkman parameter
Du	Dufour effects
Sr	Soret number
M	Hartman number
γ^*	Slip concentration parameter
E	Energy activation energy parameter
α_0	Inclination of channel
T_1, C_2	Temperature and concentration on walls
λ_1, λ_2	Ration of relaxation to retardation time.

Symbols	*Interpretation*
$(\overline{U}, \overline{V})$	Velocity component in a fix frame
$(\overline{u}, \overline{v})$	Velocity component in a moving frame
H_1, H_2	Wall shaped in a fix frame
B	Magnetic Field
B_0	Constant transverse magnetic field
λ	Wave length
φ_1	Phase difference
β_1, β_2	Coefficient of thermal and concentration expansion
κ_1	Porous medium permeability
μ	Dynamic viscosity
T, C	Liquids temperature and concentration
K_T	Thermo diffusion ratio
k_r^2	Rate of Chemical reaction
n	Fitted rate constant
τ	Cauchy stress tensor
I	Identity tensor
$\frac{d}{dt}$	Material derivative.
m	Hall number
δ	Wave parameter
Pr	Prandtl parameter
Re	Reynolds parameter
Da	Darcy parameter
Sc	Schmidt parameter
a^*	Velocity slip parameter
Gc, Gr	Mass and thermal Gashrof number
ψ	Stream function

ξ	Chemical reaction parameter
θ, ψ	Dimensionless temperature and concentration respectively
β^*	Thermal slip parameter

1. Introduction

Fluid motion through peristaltic activity has extensively present in various industrial, environment, geophysics and physiological processes. For instance, peristaltic activity includes swallowing of food particles via oesophagus, chyme delivery (an acidic fluid) through gastrointestinal tract, body waste transportation from urinary organ to bladder, passage of blood in tiny blood vessels, blood transportation from heart to other body organs, toxic, sanative and corrosive materials transportation, from the root of trees to its every branch and leaves water is transported through peristaltic movement and in various other's. Noticing all these aforementioned uses of peristalsis various researchersrs are presented the peristaltic activity through experimentally and theoretically. Latham [1] was the very first researcher who examined the fluid movement by peristaltic principle numerically. Shapiro et al. [2] verified the results of Latham [1] theoretically by considering lubrication assumption. Peristaltic activity is explored by various researchers (see Refs. [3–13]) for linear and non-linear fluid models by considering no slip and partial slip effects after the pioneering attempts of Latham [1] and Shapiro et al. [2].

Fluid flows affected by mixed convection aspects are due to the mix of forced and free convections combination. These kinds of flows have vital presence in numerous fields of industry & engineering. Such as, geological, astrophysics, in electronic devices cooling, lubricated technologies, furnaces, fireplace control, metallurgical industry and etc. All these application and importance of convective nanofluid flows in various industrial and engineering processes via peristalsis boosts the interest of researchers towards the field. Thus Srinivas et al. [14], Mustafa et al. [15], Srinivas and Muthuraj [16] and Abbasi et al. [17], examined the mix convective peristaltic flow with various assumptions through different channels (i.e., symmetric/asymmetric/non-uniform). Also, the mixed convective flow aspects in nanomaterials becomes more prominent in various engineering processes such as cooling and heating thermal equipment's, solar energy in thermal processes, boilers, in maintaining nuclear reactors temperature, refrigerator's, electronic and automobile vehicles and in several others. These uses of mixed convective in peristalsis of nano liquids motivates the researchers to examine the mix convective nanofluids to understand its dynamics (see few researchers [18–22]). Furthermore in past few years many researchers have studied about the nanofluid flow under the assumptions of nonlinear mixed convection, diffusion of oxygen and hydro liquid, Eyring-Powell in asymmetric channel (see few researchers [23–31]).

Material flows through various physiological organs likely, in gall bladder having stone, in kidney, in lungs etc are the example of porous space. Thus, few latest studies [32–37] regarding peristalsis with Darcy and modified Darcy resistance effects verify the existence of porous media in above mentioned and several other applications. Magnetohydrodynamic is extensively used in drug delivery during cancer treatment, tumours detection and its treatment, convection in blood pump machines, to reduce wound through surgeries, in MRI (i.e., magnetic resonance image) to interrogate the medicine delivery and decease detection processes. Many recent scientists, physicians and researchers attracted to examine the MHD in peristaltic flow for Newtonian and non-Newtonian electrically conductive materials (see refers. [38–44]).

The previous existing literature it comes to noted that earlier there is no study on Jeffrey fluid under the assumptions of peristaltic flow, nonlinear mix convection, Joule heating and slip aspects. The arrangement of this research is as follows in section 1 introduction and historical background of the topic is explained, in section 2 problem is formulated in the form of mathematical equations, in section 3 solution procedure is discussed, in section 4 impact of parameters on flow quantities is described and in section 4 main outcomes of this study are listed.

1.1. Problem formulation

An in compressible and electrically conducting Jeffrey liquid through an asymmetric propagating inclined channel configuration is taken. The main considerations here are non-linear force and natural convection, heat generation absorption and second order momentum slip. Graphical representation shown in Fig. 1.

Mathematical form of propagating waves is given below in Eq. (1 &2):

$$H_1 = -d_2 - b_1 \cos\left[\frac{2\pi}{\lambda}(X - ct + \varphi_1)\right], \textit{Lower wave} \tag{1}$$

$$H_2 = d_1 + a_1 \cos\left[\frac{2\pi}{\lambda}(X - ct)\right], \textit{Upper wave} \tag{2}$$

Mathematical shapes of walls are mentioned in equations which govern the given flow system are [9–42]:

$$\nabla.\mathbf{V} = 0, \tag{3}$$

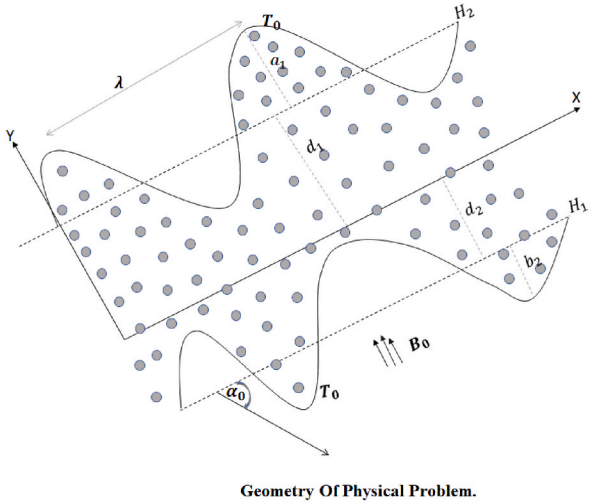

Fig. 1. Geometry of physical problem.

$$\rho\frac{d\mathbf{V}}{dt}=\nabla.\boldsymbol{\tau}+(\mathbf{J}\times\mathbf{B})-\frac{\mu}{k_1(1+\lambda_1)}\left(\mathbf{V}+\lambda_2\frac{d\mathbf{V}}{dt}\right)+ \tag{4}$$
,

$$\rho\mathbf{g}\left[\beta_1(T-T_0)+\gamma_1(T-T_0)^2\right]+\rho\mathbf{g}\left[\beta_2(C-C_0)+\gamma_2(C-C_0)^2\right]$$

$$\rho C_P\frac{dT}{dt}=k\ \nabla^2T+\mathbf{S}.\mathbf{A}+\frac{D_BK_T}{C_s}\nabla^2C+\frac{\mathbf{J}.\mathbf{J}}{\sigma}+Q_0(T-T_0)\,, \tag{5}$$

$$\frac{dC}{dt}g=D_B\ \nabla^2C+\frac{D_BK_T}{C_s}\ \nabla^2T-K_r^2(C-C_0)\left(\frac{T}{T_0}\right)^n\exp\left(-\frac{E_a}{KT}\right) \tag{6}$$

Above equations (3)–(6) in component form we have:

$$\frac{\partial V}{\partial Y}+\frac{\partial U}{\partial X}=0, \tag{7}$$

$$\rho\left[\frac{\partial U}{\partial t}+V\frac{\partial U}{\partial Y}+U\frac{\partial U}{\partial X}\right]=-\frac{\partial P}{\partial X}+\frac{\partial S_{YX}}{\partial Y}+\frac{\partial S_{XX}}{\partial X}-\frac{\mu}{k_1(1+\lambda_1)}\left(U+\lambda_2\frac{dU}{dt}\right)-$$
$$\frac{\sigma B_0^2}{1+m^2}(U-mV)$$
$$+\rho g\left(\left[\beta_1(T-T_0)+\gamma_1(T-T_0)^2\right]+\left[\beta_2(C-C_0)+\gamma_2(C-C_0)^2\right]\right)\sin\alpha_0, \tag{8}$$

$$\rho\left[\frac{\partial V}{\partial t}+V\frac{\partial V}{\partial Y}+U\frac{\partial V}{\partial X}\right]=-\frac{\partial P}{\partial Y}+\frac{\partial S_{YY}}{\partial Y}+\frac{\partial S_{XY}}{\partial X}-\frac{\mu}{k_1(1+\lambda_1)}\left(V+\lambda_2\frac{dV}{dt}\right)-$$
$$\frac{\sigma B_0^2}{1+m^2}(V+mU)$$
$$+\rho g\left(\left[\beta_1(T-T_0)+\gamma_1(T-T_0)^2\right]+\left[\beta_2(C-C_0)+\gamma_2(C-C_0)^2\right]\right)\cos\alpha_0, \tag{9}$$

$$\rho C_p\left[\frac{\partial}{\partial t}+V\frac{\partial}{\partial Y}+U\frac{\partial}{\partial X}\right]T=k\left(\frac{\partial^2}{\partial Y^2}+\frac{\partial^2}{\partial X^2}\right)T+2\left\{\begin{array}{l}\left(\frac{\partial U}{\partial Y}+\frac{\partial V}{\partial X}\right)S_{XY}\\+\frac{\partial U}{\partial Y}S_{XX}+\frac{\partial V}{\partial Y}S_{YY}\end{array}\right\}+$$
$$\frac{K_TD_B}{C_s}\left(\frac{\partial^2}{\partial Y^2}+\frac{\partial^2}{\partial X^2}\right)C+\frac{\sigma B_0^2}{1+m^2}\left(U^2+V^2\right)+Q_0(T-T_0), \tag{10}$$

$$\left[\frac{\partial}{\partial t}+V\frac{\partial}{\partial Y}+U\frac{\partial}{\partial X}\right]C=D_B\left(\frac{\partial^2}{\partial Y^2}+\frac{\partial^2}{\partial X^2}\right)C+\frac{D_BK_T}{C_s}\left(\frac{\partial^2}{\partial Y^2}+\frac{\partial^2}{\partial X^2}\right)T-$$
$$k_r^2(C-C_0)\left(\frac{T}{T_0}\right)^n\exp\left(-\frac{E_a}{KT}\right). \tag{11}$$

The stress components S_{XX}, S_{XY} and S_{YY} are expressed:

$$S_{XX}=\frac{2\mu}{1+\lambda_1}\left(1+\lambda_2\left(\frac{\partial}{\partial t}+U\frac{\partial}{\partial X}+V\frac{\partial}{\partial Y}\right)\right)\frac{\partial U}{\partial X}, \tag{12}$$

$$S_{YY}=\frac{2\mu}{1+\lambda_1}\left(1+\lambda_2\left(\frac{\partial}{\partial t}+U\frac{\partial}{\partial X}+V\frac{\partial}{\partial Y}\right)\right)\frac{\partial V}{\partial Y}, \tag{13}$$

$$S_{XY}=\frac{\mu}{1+\lambda_1}\left(1+\lambda_2\left(\frac{\partial}{\partial t}+V\frac{\partial}{\partial Y}+U\frac{\partial}{\partial X}\right)\right)\left(\frac{\partial U}{\partial Y}+\frac{\partial V}{\partial X}\right). \tag{14}$$

Boundary conditions of equations 7–11 are: [9, 44]:

$$U-\alpha^*S_{XY}-\alpha_2^*\frac{\partial S_{XY}}{\partial Y}=0, T-\beta^*\frac{\partial T}{\partial Y}=T_0, C-\gamma^*\frac{\partial C}{\partial Y}=C_0 \text{ at } Y=H_1, \tag{15}$$

$$U+\alpha^*S_{XY}+\alpha_2^*\frac{\partial S_{XY}}{\partial Y}=0, T+\beta^*\frac{\partial T}{\partial Y}=T_0, C+\gamma^*\frac{\partial C}{\partial Y}=C_0 \text{ at } Y=H_2, \tag{16}$$

Transforming system from fix (7–16) to wave frame by using (17)

$$\bar{y}=Y, \bar{x}=X-ct, \bar{v}=V, \bar{u}=U-c. \tag{17}$$

$$\frac{\partial\bar{v}}{\partial\bar{y}}+\frac{\partial\bar{u}}{\partial\bar{x}}=0, \tag{18}$$

$$\rho\left[\bar{v}\frac{\partial\bar{u}}{\partial\bar{y}}+\bar{u}\frac{\partial\bar{u}}{\partial\bar{x}}\right]=-\frac{\partial\bar{P}}{\partial\bar{x}}+\frac{\partial S_{\bar{x}\bar{x}}}{\partial\bar{x}}+\frac{\partial S_{\bar{y}\bar{x}}}{\partial\bar{y}}-\frac{\mu}{k_1(1+\lambda_1)}\left(\bar{u}+c+\lambda_2\left(\bar{v}\frac{\partial\bar{u}}{\partial\bar{y}}+\bar{u}\frac{\partial\bar{u}}{\partial\bar{x}}\right)\right)-$$
$$\frac{\sigma B_0^2}{1+m^2}(\bar{u}+c-m\bar{v})$$
$$+\rho g\left(\left[\beta_1(T-T_0)+\gamma_1^*(T-T_0)^2\right]+\left[\beta_2(C-C_0)+\gamma_2^*(C-C_0)^2\right]\right)\sin\alpha_0, \tag{19}$$

$$\rho\left[\bar{v}\frac{\partial\bar{v}}{\partial\bar{y}}+\bar{u}\frac{\partial\bar{v}}{\partial\bar{x}}\right]=-\frac{\partial\bar{P}}{\partial\bar{y}}+\frac{\partial S_{\bar{y}\,\bar{y}}}{\partial\bar{y}}+\frac{\partial S_{\bar{x}\bar{y}}}{\partial\bar{x}}-\frac{\mu}{k_1(1+\lambda)}\left[\bar{v}+\lambda_2\left(\bar{v}\frac{\partial\bar{u}}{\partial\bar{y}}+\bar{u}\frac{\partial\bar{v}}{\partial\bar{x}}\right)\right]-$$
$$\frac{\sigma B_0^2}{1+m^2}(\bar{v}+m\bar{u}+m\bar{c})+\rho g\left(\left[\beta_1(T-T_0)+\gamma_1^*(T-T_0)^2\right]+\left[\beta_2(C-C_0)+\gamma_2^*(C-C_0)^2\right]\right)\cos\alpha_0, \tag{20}$$

$$\rho C_p\left[\bar{v}\frac{\partial}{\partial\bar{y}}+\bar{u}\frac{\partial}{\partial\bar{x}}\right]T=k\left[\frac{\partial^2}{\partial\bar{y}^2}+\frac{\partial^2}{\partial\bar{x}^2}\right]T+2\left\{\begin{array}{l}\frac{\partial\bar{u}}{\partial\bar{y}}S_{\bar{x}\bar{x}}+\frac{\partial\bar{v}}{\partial\bar{y}}S_{\bar{y}\bar{y}}+\\ \left(\frac{\partial\bar{u}}{\partial\bar{y}}+\frac{\partial\bar{v}}{\partial\bar{x}}\right)S_{\bar{x}\bar{y}}\end{array}\right\}+$$
$$\frac{D_BK_T}{C_s}\left(\frac{\partial^2}{\partial\bar{y}^2}+\frac{\partial^2}{\partial\bar{x}^2}\right)C+\frac{\sigma B_0^2}{1+m^2}\left((c+\bar{u})^2+\bar{v}^2\right)+Q_0(T-T_0), \tag{21}$$

$$\left[\bar{v}\frac{\partial}{\partial\bar{y}}+\bar{u}\frac{\partial}{\partial\bar{x}}\right]C=D_B\left(\frac{\partial^2}{\partial\bar{y}^2}+\frac{\partial^2}{\partial\bar{x}^2}\right)C+\frac{D_BK_T}{C_s}\left(\frac{\partial^2}{\partial\bar{y}^2}+\frac{\partial^2}{\partial\bar{x}^2}\right)T-$$
$$k_r^2(C-C_0)\left(\frac{T}{T_0}\right)^n\exp\left(-\frac{E_a}{KT}\right), \tag{22}$$

The transformed boundary conditions yield:

$$\bar{u}+c-\alpha^*S_{\bar{x}\bar{y}}-\alpha_2^*\frac{\partial S_{\bar{x}\bar{y}}}{\partial\bar{y}}=0, T-\beta^*\frac{\partial T}{\partial\bar{y}}=T_0, C-\gamma^*\frac{\partial C}{\partial\bar{y}}=C_0 \text{ at } \bar{y}=h_1, \tag{23}$$

$$\bar{u}+c+\alpha^*S_{\bar{x}\bar{y}}+\alpha_2^*\frac{\partial S_{\bar{x}\bar{y}}}{\partial\bar{y}}=0, T+\beta^*\frac{\partial T}{\partial\bar{y}}=T_0, C+\gamma^*\frac{\partial C}{\partial\bar{y}}=C_0 \text{ at } \bar{y}=h_2, \tag{24}$$

To make the system of Eqs. 18–24 dimensionless, the non-dimensional form of quantities is expressed below

$$x=\frac{\overline{x}}{\lambda}, y=\frac{\overline{y}}{d_1}, v=\frac{\overline{v}}{c}, u=\frac{\overline{u}}{c}, \varphi=\frac{C-C_0}{C_0}, \theta=\frac{T-T_0}{T_0},$$
$$a=\frac{a_1}{d_1}, b=\frac{b_1}{d_1}, d=\frac{d_2}{d_1}, h=\frac{H}{d_1}, \delta=\frac{d_1}{\lambda}, \Pr=\frac{\mu C_p}{k}, Ec=\frac{c^2}{C_pT_0},$$
$$Br=Ec\,\Pr, \mathrm{Re}=\frac{cd_1\rho}{\mu}, Du=\frac{D_BC_0K_T}{C_pC_S\mu T_0}, Sc=\frac{\mu}{\rho D_B}, Sr=\frac{\rho D_BK_TT_0}{\mu C_0C_S}, \tag{25}$$
$$Da=\frac{k_1}{d_1^2}, M=\sqrt{\frac{\overline{\rho}}{\mu}}B_0d_1, P=\frac{d_1^2\overline{p}}{c\mu\lambda}, Gc=\frac{\rho g\beta_2C_0d_1^2}{\mu c}, Gr=\frac{\rho g\beta_2T_0d_1^2}{\mu c},$$
$$E=\frac{E_a}{kT_0}, \lambda_2=\frac{d_1\lambda_2^*}{\mu c}, \xi=\frac{d_1^2k_r^2}{\mu}.$$

Using Eq. (25), Eqs. 18–24 yields in dimensionless form as:

$$\frac{\partial v}{\partial y}+\delta\frac{\partial u}{\partial x}=0, \tag{26}$$

$$\mathrm{Re}\left[v\frac{\partial u}{\partial y}+\delta u\frac{\partial u}{\partial x}\right]=-\frac{\partial P}{\partial x}+\delta\frac{S_{xx}}{\partial x}+\frac{\partial S_{yx}}{\partial y}-\frac{M^2}{1+m^2}(u+1+mv)+$$
$$\{Gr\theta(1+\gamma_1\theta)+Gc\varphi(1+\gamma_2\varphi)\}\sin\alpha_0-\frac{1}{Da(1+\lambda)}\left[u+1+\frac{\lambda_2c}{d_1}\left(\delta u\frac{\partial u}{\partial x}+v\frac{\partial u}{\partial y}\right)\right], \tag{27}$$

$$\mathrm{Re}\delta\left[v\frac{\partial v}{\partial y}+\delta u\frac{\partial v}{\partial x}\right]=-\frac{\partial P}{\partial y}+\delta\frac{\partial S_{yy}}{\partial y}+\delta^2\frac{\partial S_{xy}}{\partial x}-\frac{\delta M^2}{1+m^2}(v+mu+m)+$$
$$\delta\{Gr\theta(1+\gamma_1\theta)+Gc\varphi(1+\gamma_2\varphi)\}\cos\alpha_0+\frac{\delta}{Da}\left[v+\frac{\lambda_2c}{d_1}\left(v\frac{\partial v}{\partial y}+\delta u\frac{\partial v}{\partial x}\right)\right], \tag{28}$$

$$\mathrm{RePr}\left[v\frac{\partial}{\partial y}+\delta u\frac{\partial}{\partial x}\right]\theta=\left(\frac{\partial^2}{\partial y^2}+\delta^2\frac{\partial^2}{\partial x^2}\right)\theta+2Br\left\{\begin{array}{l}\left(\frac{\partial u}{\partial y}+\delta\frac{\partial v}{\partial x}\right)S_{xx}+\\ \frac{\partial u}{\partial y}S_{xx}+\frac{\partial v}{\partial y}S_{yy}\end{array}\right\}+$$
$$Du\,\Pr\left[\frac{\partial^2\varphi}{\partial y^2}+\delta^2\frac{\partial^2\varphi}{\partial x^2}\right]+\frac{M^2Br}{1+m^2}\left(v^2+(u+1)^2\right)+Q\theta, \tag{29}$$

$$\mathrm{Re}\left[v\frac{\partial}{\partial y}+\delta u\frac{\partial}{\partial x}\right]\varphi=\left(\frac{\partial^2}{\partial y^2}+\delta^2\frac{\partial^2}{\partial x^2}\right)\varphi+SrSc\left[\frac{\partial^2\theta}{\partial y^2}+\delta^2\frac{\partial^2\theta}{\partial x^2}\right]+$$
$$Sc\xi\varphi(\theta+1)^n\exp\left[\frac{-E}{1+\theta}\right], \tag{30}$$

$$u-\frac{1}{1+\lambda_1}\left(\alpha\frac{\partial u}{\partial y}+\alpha_2\frac{\partial^2u}{\partial y^2}\right)=-1, \theta-\beta\frac{\partial\theta}{\partial y}=0, \varphi-\gamma\frac{\partial\varphi}{\partial y}=0, y=h_1, \tag{31}$$

$$u+\frac{1}{1+\lambda_1}\left(\alpha\frac{\partial u}{\partial y}+\alpha_2\frac{\partial^2u}{\partial y^2}\right)=-1, \theta+\beta\frac{\partial\theta}{\partial y}=0, \varphi+\gamma\frac{\partial\varphi}{\partial y}=0, y=h_2, \tag{32}$$

The new dimensionless numbers in Eqs.26–30 are

$$\gamma_1=\gamma_1^*T_0, \gamma_2=\gamma_2^*C_0, \alpha_2=, Q=\frac{Q_0d_1^2}{k}, \alpha_2=\frac{\mu\alpha_2^*}{d_1^2}. \tag{33}$$

Fluid velocities are introduced in form of stream function as

$$u=\frac{\partial\psi}{\partial y}, v=-\delta\frac{\partial\psi}{\partial x}. \tag{34}$$

By using the stream function Eq. (34) equations 26–32 becomes:

$$-\delta\frac{\partial^2\psi}{\partial x\partial y}+\delta\frac{\partial^2\psi}{\partial x\partial y}=0, \tag{35}$$

$$\mathrm{Re}\left[-\delta\frac{\partial^3\psi}{\partial x\partial y^2}+\delta\frac{\partial^3\psi}{\partial x\partial y^2}\right]=-\frac{\partial P}{\partial x}+\delta\frac{S_{xx}}{\partial x}+\frac{\partial S_{yx}}{\partial y}-\frac{M^2}{1+m^2}\left[\frac{\partial\psi}{\partial y}+1-\delta m\frac{\partial\psi}{\partial x}\right]+$$
$$\{Gr\theta(1+\gamma_1\theta)+Gc\varphi(1+\gamma_2\varphi)\}\sin\alpha_0-\tag{36}$$
$$\frac{1}{Da(1+\lambda)}\left[\frac{\partial\psi}{\partial y}+1+\frac{\lambda_2 c}{d_1}\left(\delta\frac{\partial^3\psi}{\partial x\partial y^2}+\delta\frac{\partial^3\psi}{\partial x\partial y^2}\right)\right],$$

$$\mathrm{Re}\left[-\delta^2\frac{\partial^3\psi}{\partial x^2\partial y}+\delta^2\frac{\partial^3\psi}{\partial x^2\partial y}\right]=-\frac{\partial P}{\partial y}+\delta\frac{\partial S_{yy}}{\partial y}+\delta^2\frac{\partial S_{xy}}{\partial x}-$$
$$\frac{\delta M^2}{1+m^2}\left[-\delta\frac{\partial\psi}{\partial x}+m\frac{\partial\psi}{\partial y}+m\right]+\delta\{Gr\theta(1+\gamma_1\theta)+Gc\varphi(1+\gamma_2\varphi)\}\cos\alpha_0+\tag{37}$$
$$\frac{\delta}{Da}\left[-\delta\frac{\partial\psi}{\partial x}+\frac{\lambda_2 c}{d_1}\left(\left[\delta^2\frac{\partial^3\psi}{\partial x^2\partial y}-\delta^2\frac{\partial^3\psi}{\partial x^2\partial y}\right]\right)\right],$$

$$\mathrm{RePr}\left[-\delta\frac{\partial\psi\partial\theta}{\partial x\partial y}+\delta\frac{\partial\psi\partial\theta}{\partial y\partial x}\right]=\frac{\partial^2\theta}{\partial y^2}+\delta^2\frac{\partial^2\theta}{\partial x^2}+Br\left\{\begin{array}{l}\frac{\partial\psi}{\partial y^2}S_{xx}-\delta\frac{\partial\psi}{\partial x\partial y}S_{yy}+\\ \left(\frac{\partial^2\psi}{\partial y^2}-\delta^2\frac{\partial^2\psi}{\partial x^2}\right)S_{xx}\end{array}\right\}+\tag{38}$$
$$Du\,\mathrm{Pr}\left[\frac{\partial^2\varphi}{\partial y^2}+\delta^2\frac{\partial^2\varphi}{\partial x^2}\right]+\frac{M^2Br}{1+m^2}\left(-\delta^2\frac{\partial^2\psi}{\partial x^2}+\frac{\partial^2\psi}{\partial y^2}+1\right)+Q\theta,$$

$$\mathrm{Re}\left[-\delta\frac{\partial\psi\partial\varphi}{\partial x\partial y}+\delta\frac{\partial\psi\partial\varphi}{\partial y\partial x}\right]=\frac{\partial^2\varphi}{\partial y^2}+\delta^2\frac{\partial^2\varphi}{\partial x^2}+SrSc\left[\frac{\partial^2\varphi}{\partial y^2}+\delta^2\frac{\partial^2\varphi}{\partial x^2}\right]$$
$$+Sc\xi\varphi(\theta+1)^n\exp\left[\frac{-E}{1+\theta}\right],\tag{39}$$

$$\psi=-\frac{F}{2},\frac{\partial\psi}{\partial y}-\alpha S_{xy}-\alpha_2\frac{\partial S_{xy}}{\partial y}=-1,\theta-\beta\frac{\partial\theta}{\partial y}=0,\varphi-\gamma\frac{\partial\varphi}{\partial y}=0,y=h_1,\tag{40}$$

$$\psi=\frac{F}{2},\frac{\partial\psi}{\partial y}+\alpha S_{xy}+\alpha_2\frac{\partial S_{xy}}{\partial y}=-1,\theta+\beta\frac{\partial\theta}{\partial y}=0,\varphi+\gamma\frac{\partial\varphi}{\partial y}=0,y=h_2.\tag{41}$$

By using small Reynold number and wave number $\mathrm{Re}\to0,\delta\to0,$ Eq (35) vanished identically and Eqs.36–41 becomes:

$$\frac{\partial p}{\partial x}=\frac{\partial^3\psi}{\partial y^3}\left(\frac{1}{1+\lambda_1}\right)-\frac{M^2}{1+m^2}\left[\frac{\partial\psi}{\partial y}+1\right]+\{Gr\theta(1+\gamma_1\theta)+Gc\varphi(1+\gamma_2\varphi)\}\sin\alpha_0-$$
$$\frac{1}{Da(1+\lambda_1)}\left[\frac{\partial\psi}{\partial y}+1\right],\tag{42}$$

$$\frac{\partial p}{\partial y}=0,\tag{43}$$

$$0=\frac{\partial^2\theta}{\partial y^2}+2BrS_{xy}\left[\frac{\partial^2\psi}{\partial y^2}\right]+Du\,\mathrm{Pr}\frac{\partial^2\varphi}{\partial y^2}+\frac{M^2Br}{1+m^2}\left[1+\frac{\partial\psi}{\partial y}\right]^2+Q\theta,\tag{44}$$

$$0=\frac{\partial^2\varphi}{\partial y^2}+SrSc\left[\frac{\partial^2\theta}{\partial y^2}\right]+Sc\xi\varphi(\theta+1)^n\exp\left[\frac{-E}{1+\theta}\right].\tag{45}$$

$$\psi=-\frac{F}{2},\frac{\partial\psi}{\partial y}-\frac{1}{1+\lambda_1}\left(\alpha\frac{\partial^2\psi}{\partial y^2}-\alpha_2\frac{\partial^3\psi}{\partial y^3}\right)=-1,\theta-\beta\frac{\partial\theta}{\partial y}=0,\varphi-\gamma\frac{\partial\varphi}{\partial y}=0,y=h_1,\tag{46}$$

$$\psi=\frac{F}{2},\frac{\partial\psi}{\partial y}+\frac{1}{1+\lambda_1}\left(\alpha\frac{\partial^2\psi}{\partial y^2}+\alpha_2\frac{\partial^3\psi}{\partial y^3}\right)=-1,\theta+\beta\frac{\partial\theta}{\partial y}=0,\varphi+\gamma\frac{\partial\varphi}{\partial y}=0,y=h_2.\tag{47}$$

Using compatibility assumption, we get from Eqs. (42) and (43):

$$\frac{\partial^2}{\partial y^2}\left(\frac{1}{1+\lambda_1}\frac{\partial^2\psi}{\partial y^2}\right)-\frac{M^2}{(1+m^2)}\frac{\partial^2\psi}{\partial y^2}+\{Gr\theta(1+\gamma_1\theta)+Gc\varphi(1+\gamma_2\varphi)\}\sin\alpha_0-\frac{1}{Da(1+\lambda_1)}\frac{\partial}{\partial y}\left[1+\frac{\partial\psi}{\partial y}\right]=0, \tag{48}$$

1.1.1. Solution methodology

As the system of Eqs. (44), (45) and (48) are coupled and nonlinear, thus to evaluate their exact/analytic solution seems complex. So the numerical way is used to evaluate the solution of this system of equation subject to the boundary conditions (46 & 47). Here the built-in numerical technique is used called NDSolve in Mathematica software. Such numerical built-in numerical technique is working under the algorithms of shooting and RK-Felburgh numerical methods.

1.1.2. Result and discussion

This section is devoted to study the results of velocity u, temperature θ and concentration φ against pertinent quantities. Figs 2–17 with fixed values of $(a=0.3, x=0, m=1, Gr=1, Gc=1, \alpha 1=\frac{\pi}{4}, \Pr=1, \Omega=1, b=0.5, \varphi_1=\frac{\pi}{4})$ are organized to study the physical versions of flow quantities against all the influential sundry quantities respectively.

1.1.3. Axial velocity profile

Figs (2-7) demonstrates the effects of large magnetic parameter M, relaxation to retardation quantity λ_1, velocity slip parameters α and α_2 of first and second order respectively, non-linear thermal and concentration mix convective γ_1 and γ_2 parameters on velocity u. As the momentum equation is of parabolic kind due to such characteristic's velocity curves are also behave like parabola. Fig (2) depicts the reduction in velocity u at centre and in the vicinity of boundary it increases for increasing M. Decrease in velocity is because of a resistive force known as Lorentz force also magnetic field changes the direction of velocity. Larger magnetic field impact strengthens the Lorentz force effects. Relaxation to retardation quantity λ_1 effects on axial velocity are captured in Fig (3). This plot describes the situation when Jeffery fluid moves from relaxation to retardation. It is well known fact that the larger relaxation time fluids have higher temperature and concentration and smaller relaxation time fluids possess lower temperature and concentration. It is a physical phenomenon of stress and strain because of the consistent behavior of viscoelastic fluid on thermodynamic principles here the fluid velocity u becomes decreasing at the channel centre while it escalates towards the walls. Figs (4 and 5) relocates that both

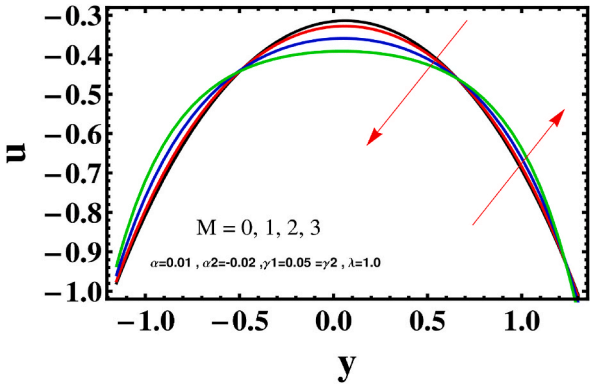

Fig. 2. Velocity ***u for M***.

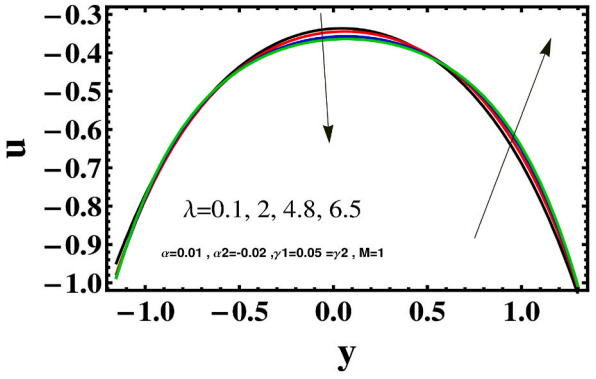

Fig. 3. Velocity ***u for*** λ.

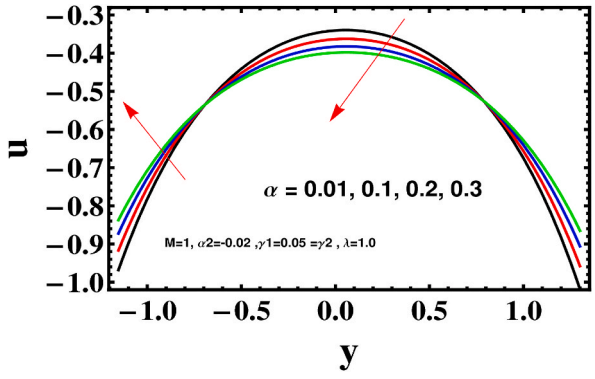

Fig. 4. Velocity **u for α**.

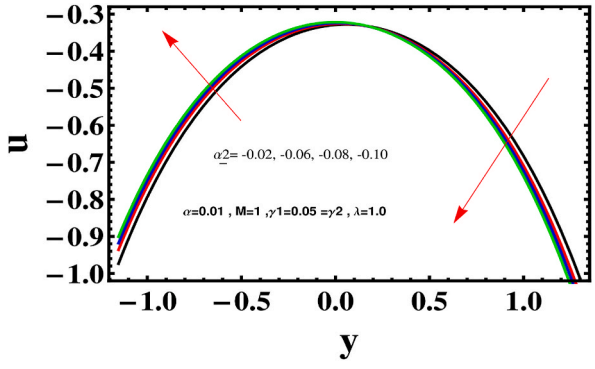

Fig. 5. Velocity **u for α_2**.

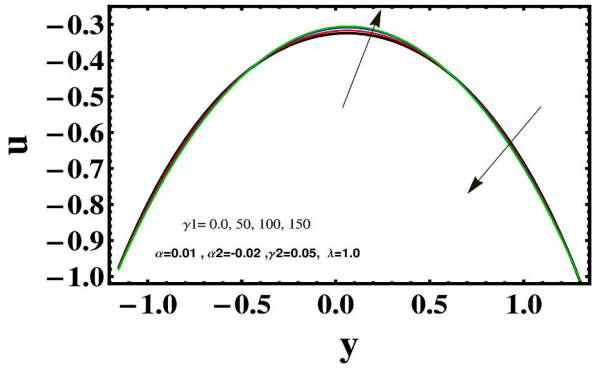

Fig. 6. Velocity **u for γ_1**.

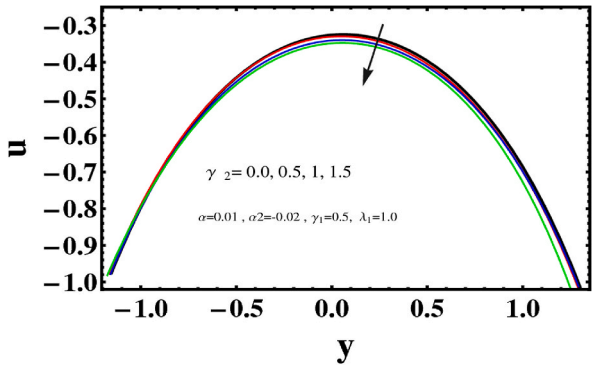

Fig. 7. Velocity **u for γ_2**.

the slip parameters α and α_2 assists the velocity near boundaries and dominates it at channel centre. Fig (6–7) illustrate that larger non-linear thermal γ_1 and concentration γ_2 mix convection parameters have opposite impacts on velocity u. It is because of the non-linearity and buoyance forces (applied on a fluid then collision in a particles are decreases and energy among them decreases therefore velocity is increases) and (concentration is increases as the diffusion is decreases conversely diffusion among the particles is increases and concentration is decreases) which affects the velocity at both centre and walls.

1.1.4. *Temperature profile*

This subsection featuring the effects of heat generation/absorption Q, thermal slip quantity β, Dufour effects Du, dissipation Br and Soret Sr effects on temperature θ through Figs 8–12. Through Fig (8) it comes to know that for heat generation (i.e for positive Q) produced by thermal radiation is increased, it breaks the bond that holds fluid particles, thus fluid dissipates the fluid particles energy

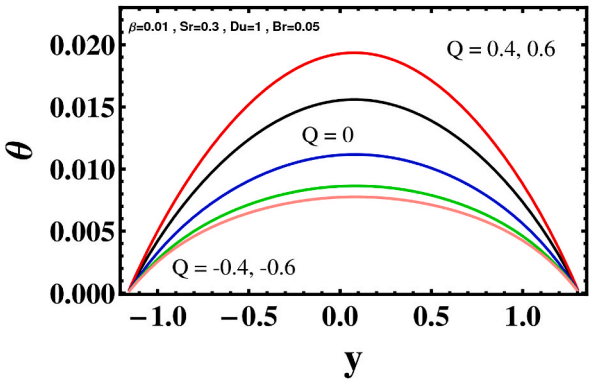

Fig. 8. Temperature θ *for* Q.

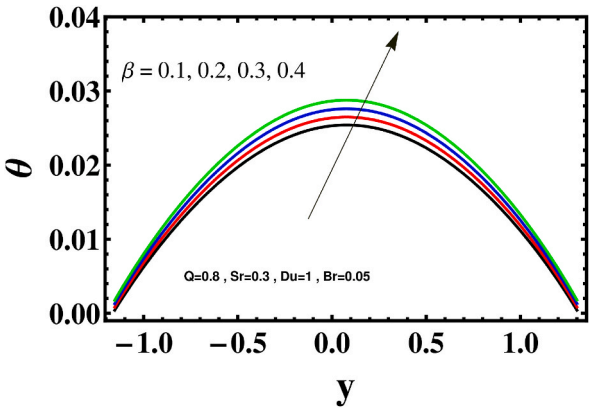

Fig. 9. Temperature θ *for* β.

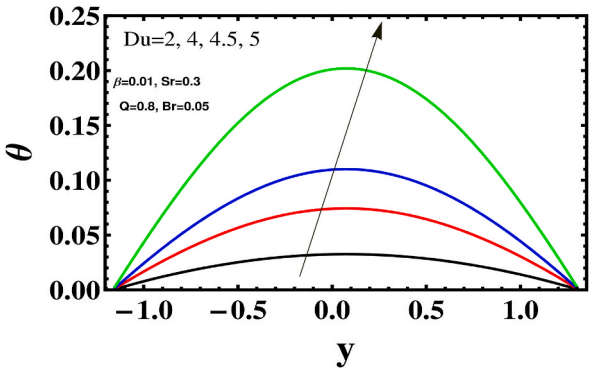

Fig. 10. Temperature θ *for* Du.

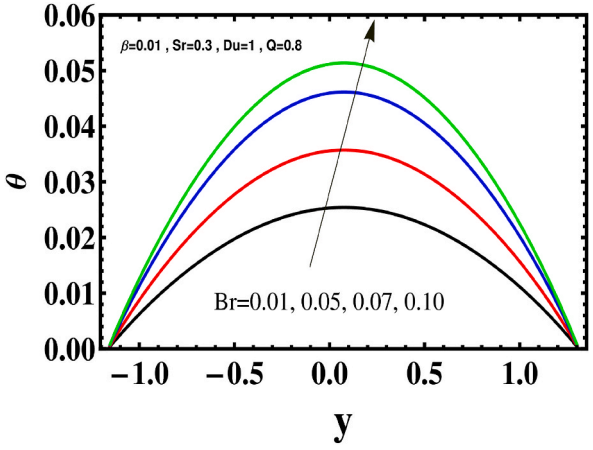

Fig. 11. Temperature θ *for Br*.

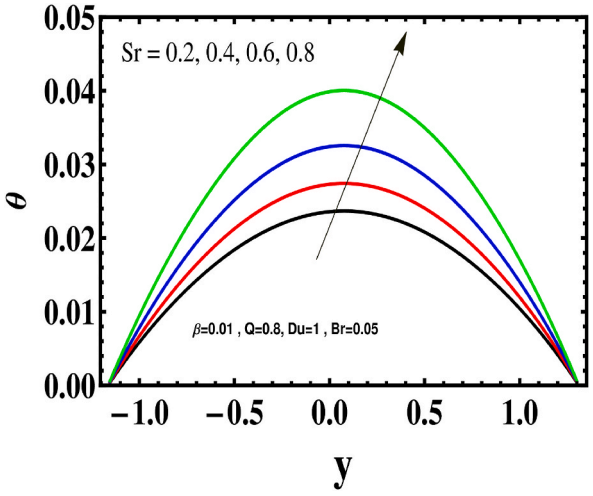

Fig. 12. Temperature θ *for Sr*.

due to this temperature increases whereas for heat absorption (i.e for negative Q) temperature is started decreasing. Fig (9) illustrates that due to thermal slip β effects fluid particles at channel walls transfer their energy through convection which strengthen the fluid temperature towards the channel centre as the value of thermal parameter increases, the thermal boundary layer thickness decreases even when a small amount of heat is transferred to the fluid from the channel. Dufour Du effects on temperature are incorporated

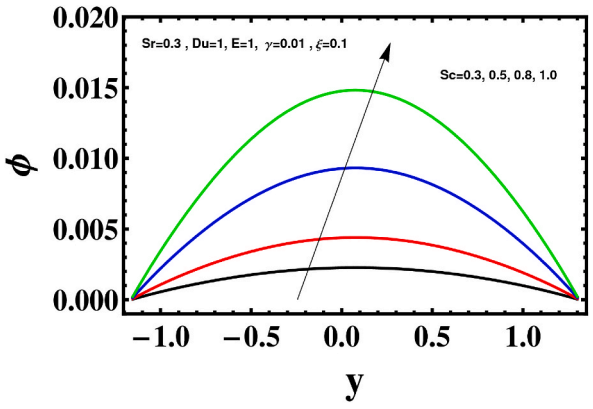

Fig. 13. Concentration φ *for Sr*.

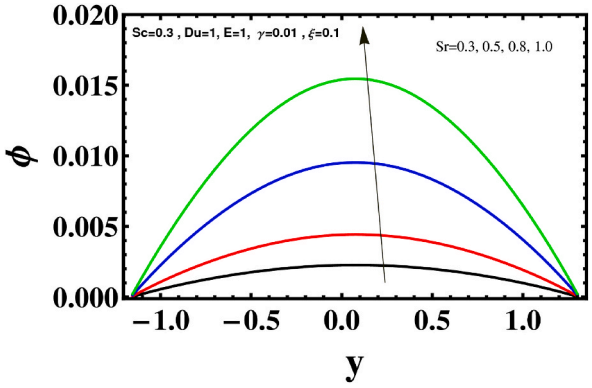

Fig. 14. Concentration *φ for Sc*.

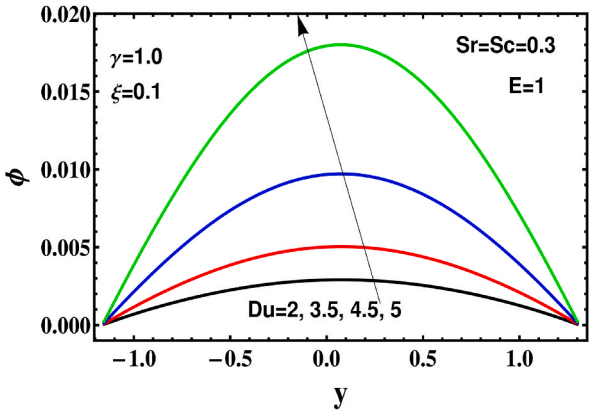

Fig. 15. Concentration *φ for Du*.

through Fig (10). Dufour effect of flux is due to the composition gradient and thermos effect because of collision of particle increases and energy among them decreases so temperature is increases. Increasing Dufour enhance the temperature profile because Dufour *Du* and temperature have directly proportional relation with each other. As it is obvious that larger dissipation *Br* effects depends upon on viscosity as viscosity is increased the resistance between material particles also increases which assists the fluid particles to lost their energy in huge amount. This is the physical fact behind the enhancement in temperature for huge *Br* (see Fig (11)). Soret *Sr* effects on temperature are captured in Fig (12). As the viscosity is inversely proportional to *Sr* number, thus for higher *Sr* viscosity of material deduces which escalates the fluid motion, in response temperature also escalates due to faster motion of fluid particle.

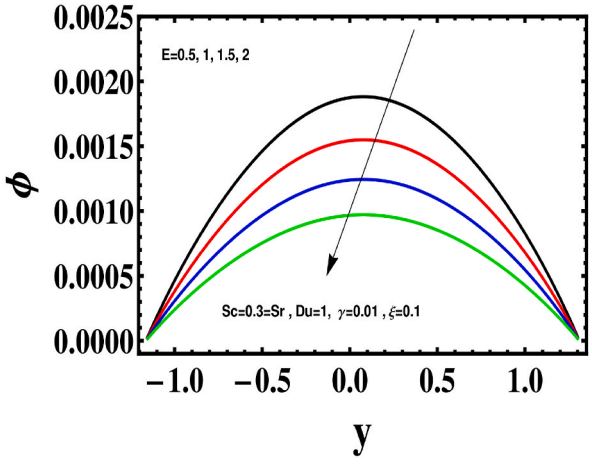

Fig. 16. Concentration *φ for E*.

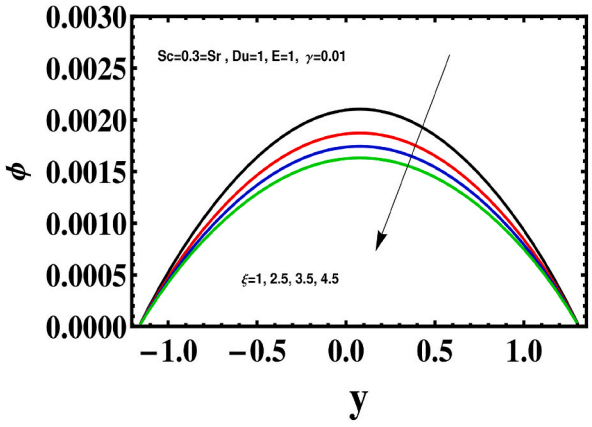

Fig. 17. Concentration φ *for* ξ.

1.1.5. Concentration profile

Figs (13 −17) depicts the concentration φ behaviour against Schmidt *Sc* parameter, Soret *Sr* number, Dufour *Du* parameter, activation energy *E* and chemical reaction parameter ξ. Figs (13 −15) illustrates the *Sc*, *Sr* and *Du* impacts on fluid concentration φ. It is evident through mathematic expression of *Sc*, *Sr* and *Du* that these numbers have inverse relation with fluid viscosity. Thus, when effects of these quantities increase viscosity of Jeffery fluid is decreased, Fig (16) clearly depicts the energy activation parameter *E* impacts on concentration. This Fig determines that increasing energy activation *E* parameter means the collision among the particles is increases and energy is decreases therefore decrease the material concentration. Dominating impacts of chemical reaction parameter on concentration are enclosed in Fig (17).

2. Conclusions

The outcomes of this study are.

- Opposite response of velocity is depicted against non-linear thermal and concentration mix convection parameters.
- Velocity shows reverse behaviour for second order momentum slip.
- Temperature enhances for heat generation and decays for heat absorption effects.
- Chemical reaction and activation energy deduces the fluid concentration.

Data availability statement

No data was used for the research described in the article.

CRediT authorship contribution statement

S. Farooq: Conceptualization, Investigation, Writing – original draft, Supervision. **T. Shoaib:** Methodology, Writing – original draft, Software. **S.Z.B. Bukhari:** Formal analysis, Software. **A.S. Alqahtani:** Investigation, Validation, Writing – review & editing. **M. Y. Malik:** Conceptualization, Supervision. **S. Abdullaev:** Validation, Writing – review & editing. **S.E. Alhazmi:** Validation, Writing – review & editing.

Declaration of competing interest

The authors declare that they have no known competing financial interests or personal relationships that could have appeared to influence the work reported in this paper.

Acknowledgment

The authors extend their appreciation to the Deanship of Scientific Research at King Khalid University for funding this work through Large Groups Project under grant number RGP–2-114/1444.

References

[1] T.W. Latham, Fluid Motion in a Peristaltic Pump, MIT, Cambridge MA, 1996.
[2] A.H. Shapiro, M.Y. Jaffrin, S.L. Weinberg, Peristaltic pumping with long wavelength at low Reynolds number, J. Fluid Mech. 37 (1969) 799–825.

[3] T. Hayat, Y. Wang, K. Hutter, S. Asghar, A.M. Siddiqui, Peristaltic transport of an Oldroy-B fluid in a planner channel, Math. Probl Eng. 4 (2004) 347–376.
[4] L.M. Srivastava, V.P. Srivastava, Peristaltic transport of a power law fluid: applications to the ductus afferents of the reproductive tract, Rheol. Acta 27 (1988) 428–433.
[5] T. Hayat, N. Ali, On mechanism of peristaltic flows for power- law fluid, Phy. A 371 (2006) 188–194.
[6] H.S. Lew, Y.C. Fung, C.B. Lowenstein, Peristaltic carrying and mixing of chime, J. Biomech. 4 (1971) 297–315.
[7] T. Hayat, S. Farooq, B. Ahmad, A. Alsaedi, Homogeneous-heterogeneous reactions and heat source/sink effects in MHD peristaltic flow of micropolar fluid with Newtonian heating is a curved channel, J. Mol. Liq. 223 (2016) 469–488.
[8] K. Vajravelu, S. Sreenadh, V.R. Babu, Peristaltic transport of a Herschel-Buckley fluid in an inclined tube, Int. J. Non-linear Mech. 40 (2005) 83–90.
[9] T. Hayat, A.A. Khan, F. Bibi, S. Farooq, Activation energy and non-Darcy resistance in magneto peristalsis of Jeffrey material, J. Phy. Chem. Solids. 129 (2019) 155–161.
[10] F. Hussain, R. Ellahi, A. Zeeshan, K. Vafai, Modelling study on heated couple stress fluid peristaltically conveying gold nanoparticles through coaxial tubes; a remedy for gland tumors and arthritis, J. Mol. Liq. 268 (2018) 149–155.
[11] H. Alolaiyan, A. Riaz, A. Razaq, N. Saleem, A. Zeeshan, M.M. Bhatti, Effects of double diffusion convection on third grade nanofluid through a curved compliant peristaltic channel, Coatings 10 (2020) 154.
[12] A. Riaz, T. Abbas, A. Zeeshan, M.H. Doranehgard, Entropy generation and MHD analysis of a nanofluid with peristaltic three-dimensional cylindrical enclosures, Int. J. Numeri. Methods Heat Fluid Flow. 31 (2021) 2698–2714.
[13] A. Zeeshan, A. Riaz, F. Alzahrani, A. Moqeet, Flow analysis of two layers nano/Johnson-Segalmann fluid in blood vessel like tube with complex peristaltic wave, Math. Prob. Eng. 6 (2022) 1–18.
[14] S. Srinivas, R. Gayathri, M. Kothandapani, Mixed convective heat and mass transfer in an asymmetric channel with peristalsis, Commun. Nonlinear Sci. Numer. Simulat. 16 (2011) 1845–1846.
[15] M. Mustafa, S. Abbasbandy, S. Hina, T. Hayat, Numerical investigation on mixed convection peristaltic flow of fourth grade fluid with Soret and Dufour effects, J. Taiwan Inst. Chem. Eng. 45 (2014) 308–316.
[16] S. Srinivas, R. Muthuraj, Effects of chemical reaction and space porosity on MHD mixed convective flow in a vertical asymmetric channel with peristalsis, Math. Comput. Model. 54 (2011) 1213–1227.
[17] F.M. Abbasi, T. Hayat, A. Alsaedi, Effects of inclined magnetic field and Joule heating in mixed convective peristaltic transport of non-Newtonian fluids, Bull. Pol. Acad. Sci. Tech. Sci. 63 (2015) 501–514.
[18] S. Akram, Q. Afzal, E.H. Aly, Half-breed effects of thermal and concentration convection of peristaltic pseudoplastic nanofluid in a tapered channel with induced magnetic field, Case Study. Thermal Eng. 22 (2020), 100775.
[19] S. Munawar, N. Saleem, Mixed convective cilia triggered stream of magneto ternary nanofluid through elastic electroosmotic pump: a comparative entropic analysis, J. Mol. Liq. 352 (2022), 118662.
[20] A. Sharma, D. Tripathi, A.K. Tiwari, Analysis of double diffusive convection in electroosmosis regulated peristaltic transport of nanofluids, Physica A: Statistical Mech. Applica. 535 (2019), 122148.
[21] S. Farooq, T. Hayat, A. Alsaedi, B. Ahmad, Numerically framing the features of second order velocity slip in mixed convective flow of Sisko nanomaterial considering gyrotactic microorganisms, Int. J. Heat Mass Transf. 112 (2017) 521–532.
[22] T. Hayat, F.M. Abbasi, M. Al-Yami, S. Monaquel, Slip and Joule heating effects in mixed convection peristaltic transport of nanofluid with Soret and Dufour effects, J. Mol. Liq. 194 (2014) 93–98.
[23] P.M. Patil, M. Kulkarni, Nonlinear mixed convective nanofluid flow along moving vertical rough plate, Rev. Mex. Fis. 66 (2022) 153–161.
[24] P.M. Patil, A. Shankar, P.S. Hiremath, E. Momoniat, Nonlinear mixed convection nanofluid flow about a rough sphere with the diffusion of liquid hydrogen, Alex. Eng. J. 60 (2021) 1043–1053.
[25] P.M. Patil, H.F. Shankar, M.A. Sheremet, Nonlinear mixed convection flow over a moving yawed cylinder Driven by Buoyancy, Mathematics 9 (2021) 1275.
[26] P.M. Patil, M. Kulkarni, J.R. Tonannavar, A computational study of the triple-diffusive nonlinear convective nanofluid flow over a wedge under convective boundary constraints, Int. J. Communic. Heat Mass Transf. 128 (2021), 105561.
[27] P.M. Patil, M. Kulkarni, A numerical study on MHD double diffusive nonlinear mixed convective nanofluid flow around a vertical wedge with diffusion of liquid hydrogen, J. Egypt. Math. Soc. 29 (1–18) (2021) 24.
[28] P.M. Patil, H.F. Shankar, M.A. Sheremet, Influence of liquid hydrogen diffusion on nonlinear mixed convective circulation around a yawed cylinder, Symmetry 14 (2022) 337.
[29] P.M. Patil, M. Kulkarni, MHD quadratic mixed convection Eyring-Powell nanofluid flow with multiple diffusions, Chinese J. Phy. 77 (2022) 393–410.
[30] P.M. Patil, H.F. Shanker, Mixed convection of Silica-Molybdenum Disulphide/water hybrid nano liquid over a rough sphere, Symmetry 13 (2021) 236.
[31] P.M. Patil, S.H. Daddagoudar, P.S. Hiremath, Impacts of surface roughness on mixed convection nano fluid flow with liquid hydrogen/nitrogen diffusion, Int. J. Numer. Methods Heat Fluid Flow 29 (2019) 2146–2174.
[32] (a) S.K. Pandey, M.K. Chaube, Effect of magnetic field on peristaltic transport of couple stress fluids through a porous medium, J. Biol. Syst. 19 (2011) 251–262; (b) A.M. Abd-Alla, S.M. Abo-Dahab, H.D. El-Shahrany, Effects of rotation and magnetic, field on the nonlinear peristaltic flow of a second-order fluid in an asymmetric, channel through a porous medium, Chin. Phys. B 22 (2013), 074702.
[33] S.R. Mahmoud, N.A.S. Afifi, H.M. Al-Isede, Effect of porous medium and magnetic, field on peristaltic transport of a Jeffrey fluid, Int. J. Math. Anal. 5 (2011) 1025–1034.
[34] N.T. El-Dabe, G. Ismail, F.O. Darwesh, Peristaltic transport of a magneto non-Newtonian fluid through a porous medium in a horizontal finite channel, IOSR J. Math. 8 (2013) 32–39.
[35] M.M. Bhatti, A. Zeeshan, R. Ellahi, G.C. Shit, Mathematical modeling of heat and mass transfer effects on MHD peristaltic propulsion of two-phase flow through a Darcy-BrinkmanForchheimer porous medium, Adv. Powder Tech. 29 (2018) 1189–1197.
[36] T. Hayat, F. Bibi, S. Farooq, A.A. Khan, Nonlinear radiative peristaltic flow of Jeffrey nanofluid with activation energy and modified Darcy's law, J. Brazilian Society Mech. Sci. Eng. 41 (2019) 296.
[37] K. Ramesh, M. Devakar, Magnetohydrodynamic peristaltic transport of couple stress fluid through porous medium in an inclined asymmetric channel with heat transfer, J. Magn. Magn Mater. 394 (2015) 335–348.
[38] S. Farooq, M. Awais, M. Naseem, T. Hayat, B. Ahmad, Magnetohydrodynamic peristalsis of variable viscosity Jeffrey liquid with heat and mass transfer, Nuclear Eng. Tech. 49 (2017) 1396–1404.
[39] M.M. Bhatti, A. Zeeshan, R. Ellahi, Simultaneous effects of coagulation and variable magnetic field on peristaltically induced motion of Jeffrey nanofluid containing gyrotactic microorganism, Microvasc. Res. 110 (2017) 32–42.
[40] M.M. Bhatti, A. Zeeshan, R. Ellahi, N. Ijaz, Heat and mass transfer of two-phase flow with Electric double layer effects induced due to peristaltic propulsion in the presence of transverse magnetic field, J. Mol. Liq. 230 (2017) 237–246.
[41] T. Hayat, H. Zahir, A. Tanveer, A. Alsaedi, Soret and Dufour effects on MHD peristaltic transport of Jeffrey fluid in a curved channel with convective boundary conditions, PLoS One 12 (2017), 0164854.
[42] A.A. Khan, F. Masood, R. Ellahi, M.M. Bhatti, Mass transport on chemicalized fourth-grade fluid propagating peristaltically through a curved channel with magnetic effects, J. Mol. Liq. 258 (2018) 186–195.
[43] A. Raja, A.A. Bhise, A. Kulkarni, Entropy analysis of the MHD Jeffrey fluid flow in an inclined porous pipe with convective boundaries, I. J. of thermos-fluids 17 (2023), 100275.
[44] M. Yasin, S. Hina, R. Naz, A modern study on peristaltically induced flow of maxwell fluid considering modified, Daracy's law and Hall effect with slip condition 76 (2023) 835–850.